A new methodology for health monitoring of cable-stayed bridges; identifying the major features sensitive to damage/failure

Mohammad Hashemi Yekani, Omid Bahar

***Abstract*— In this research a general methodology is presented for health monitoring of cable-stayed bridges. This methodology has two main phases: 1) identifying different damage/failure modes through linear static, nonlinear static and nonlinear dynamic time history analyses; 2) individualizing the features of the considered bridge sensitive to the recognized damage/failure modes.**

In order to evaluate the proposed methodology as an exemplified the Kobe earthquake is normalized into 1g in the vertical, transversal and longitudinal directions and used as the input of non-linear dynamic time history analyses of the QINGZHOU Bridge. The components are divided into a few shorter frequency ranges. The features and their values sensitive to damages/failures are recognized in each individual frequency domain. Extensive analysis using various earthquake records, the Big Bear, Chi-Chi and El-Centro earthquake records, shows that expected damages and recognized sensitive features in similar frequency domains are exactly the same as those for the Kobe earthquake. Recognized sensitive features in this study are the vertical displacement and acceleration of the main span center, lateral displacement of the top of towers, vertical displacement of some points of the main girder of deck near the towers and also strain of cables. Extensive analysis shows that by using the new proposed methodology and monitoring a few selected features of a cable-stayed bridge various source of its potential damages during strong ground motions are trustfully predicted and controlled in early steps.

***Index Terms*— health monitoring, features sensitive to damage, cable-stayed bridge, nonlinear dynamic time history analyses.**

I. INTRODUCTION

Cable-stayed bridges have been widely used all over the world in the recent decades because of their remarkable advantages such as aesthetic appearance and efficient usage of structural material. Rapid progress of analysis and design procedure, high strength materials, as well as development of efficient construction techniques, lead engineers to erect long span cable-stayed bridges over 1000 m. but, on the other hand cable-stayed bridges are highly sensitive to dynamic loads such as wind, earthquake and traffic because of which they may behave beyond their service limits, or their elements exceed yield limits. Intensive loadings may cause nonlinear behavior of each part of the bridge which may be due to both material and geometric nonlinearities. Sources of these problems include sag effect of inclined cables, the effects of interaction between axial loads and bending moments in the girders and towers, large displacements effects, nonlinear stress-strain behavior of materials, and so on. In these cases, different parts of cable-stayed bridges, includes towers, cables, and main girders experience minor to major damages. Moreover, some parts of the bridge may be partially or completely collapsed. Therefore, it is crucial to monitor the behavior of such bridges to recognize all potential damage sources concerning various strong winds or earthquakes. Therefore, it is necessary to establish a monitoring system that can collect data on dynamic response of the bridge. The better the modeling and considering nonlinear sources are the more knowledgeable judgment about potential damages will be obtained. So, performing different types of analysis on the earthquakes with various characteristics is crucial for better understanding the performance of such bridges. Since, bridges play an essential role in the highway network, structural health monitoring has been implemented for recognizing the bridge behavior under different loadings. The dynamic behaviors of major components of bridge, caused by environmental loadings, are identified by full and large-scale testing. In this view point, structural health monitoring has become an important part in the design, construction and structural safety of bridges [1]–[3]. Damage/failure of main girders and towers of cable-stayed bridges is another important feature in the long span bridges [4]. This feature should be monitored to prevent bridge damage caused by external excitations such as earthquake, strong wind, differential settlement, fatigue/defect of material and loose of tension within the cables. As cable-stayed bridge with long span usually plays role in the hazard mitigation, it is very important to remain functional after moderate earthquake. Therefore, rapid structure health diagnosis is essential for cable-stayed bridge in a maintenance procedure [5]-[7]. In this paper a general methodology is presented for health monitoring of cable-stayed bridges through recognizing major features sensitive to damage/failure modes.

Nonlinear analysis is applied in studying cable-stayed bridges due to the rapid incremental development of central span lengths in such bridges. Therefore, nonlinear analyzing of these bridges is very essential for recognizing the stresses and deformations caused by external excitations. In the last decade the researchers have intensively studied the dynamic behavior and seismic responses of these highly nonlinear structures. They focused on 2D or 3D structures, all focusing on the cable-stayed bridges and their dynamic behavior characterizations excited by traffic, wind and earthquakes [8]-[9].

In order to analyze the earthquake response of cable-stayed bridges precisely, it is necessary to know their dynamic

Mohammad Hashemi Yekani ,PhD Candidate, Department of Civil Engineering, Collage of Engineering, Tehran Science and research Branch, Islamic Azad University, Tehran, Iran,+989121392049

Omid Bahar, Assistant Prof., Structural Dynamics Dept., International Institute of Earthquake Engineering and Seismology (IIEES), Tehran, Iran,+989122195967

characteristics, including modal frequencies, mode shapes and modal damping ratios. On the one hand, many papers have been published about 2D geometric nonlinear seismic response time history analysis of cable-stayed bridges [12]; some others hand have concerned 3D geometric nonlinear response of long span cable-stayed bridges during earthquake [10],[11],[13]. Ambient vibration measurements are used widely to challenge the modal analyses of real bridges [14]. Cable supported bridges have been analyzed subjecting to asynchronous longitudinal and lateral ground motions. Several researchers studied soil-structure interaction for long span cable-stayed bridges [16]. None of these researchers include all nonlinearity sources. Nonlinear dynamic analysis is the key tool of the methodology presented in this research for step by step identification of seismic response behavior of long span cable-stayed bridges. This methodology considers both geometric and material nonlinearities.

In this study a general methodology is presented for health monitoring of cable-stayed bridges through recognizing major features sensitive to their damage/failure modes. The methodology includes two main phases: 1) identifying different damage/failure modes through linear static analysis, nonlinear static analysis and nonlinear dynamic time history analysis; 2) individualizing the major features sensitive to damage/failure. In order to generalize the dynamic analysis, the selected strong ground motion earthquakes are normalized and filtered into a few given frequency ranges. In this approach, the effective features and their proper ranges are distinguished as the main tools in monitoring process of cable-stayed bridges. Accordingly, the potential damages are trustfully predicted and controlled by monitoring a few points of bridges

II. Methodology of Determining the Parameters Sensitive to Damage

The new proposed methodology attempts to consider potential damages/failures by determining the exact frequency range of the earthquakes. Eventually, the features sensitive to these recognized damages are identified. The structural elements will remain in their elastic limits by controlling the determined points precisely. In this way, the potential damages and probable collapse would be predictable.

Non-linear dynamic time-history analyses are used as the key tools for detecting the damage extent. In order to evaluate the proposed methodology as an exemplified the Kobe earthquake is used as the input of non-linear dynamic time history analyses of the QINGZHOU cable-stayed bridge. The methodology is conducted in two phases:

1) Kobe earthquake is normalized to 1 g in the vertical, longitudinal and transversal directions. Then the earthquake is filtered according to the frequency range of the cable-stayed bridge. The frequency range of the earthquake record is divided into 0-3, 3-6, 6-9, 9-12 and 12-15 Hz, which is covered about 90 modes of the QINGZHOU cable stayed-bridge. In this way, all the damage/failure modes of the bridge corresponding directly to a specific frequency ranges are determined. After filtering the earthquakes, the analyses will be conducted, and the filtered earthquakes will be applied on the structure in vertical, longitudinal and transversal directions. 2) The features and their values sensitive to damages/failures are recognized in each individual frequency domain. After initial studying of the structure's status, if the structure has not yet entered the inelastic limits, the structure is analyzed again by applying much more intense earthquakes. The analyses are continued up to observe some damages and finally failure mode of the bridge [17].

Figure 1 shows the earthquake acceleration values, the increased earthquake input applied on the structure to cause damage, and concerning excitation modes of the bridge in each frequency range. For example, concerning Kobe earthquake, the input earthquake should be 16 times greater than the main filtered earthquake in the frequency range of 12-15, in order to collapse the structure.

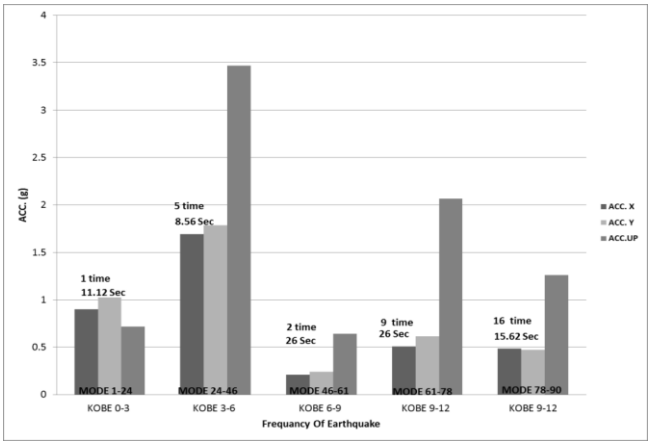

Fig. 1: The acceleration values increased input earthquakes

The damages, ordinarily observed in the conducted analyses, are related to the cables, towers and deck or a combination of them. The damage boundary as well as the limitation in which the structure shows inelastic behavior is determined by controlling the displacement center of main span and identifying its exact domain. Other criteria are: root mean square of acceleration of main span center, lateral displacement of top of the tower, vertical displacement of some points of the main girder of deck (area 3 in region II and III, Fig. 20) near the towers and cables strain. Figure 2 shows all steps of choosing, normalizing and filtering the input earthquakes in the proposed frequency ranges. Figure 3 shows the steps of analyzing and determining potential damages in the dominant frequency range, identifying the features sensitive to damage and monitoring the structure.

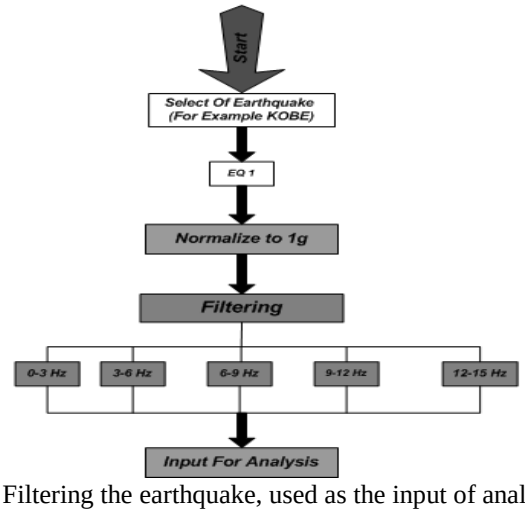

Fig. 2: Filtering the earthquake, used as the input of analysis

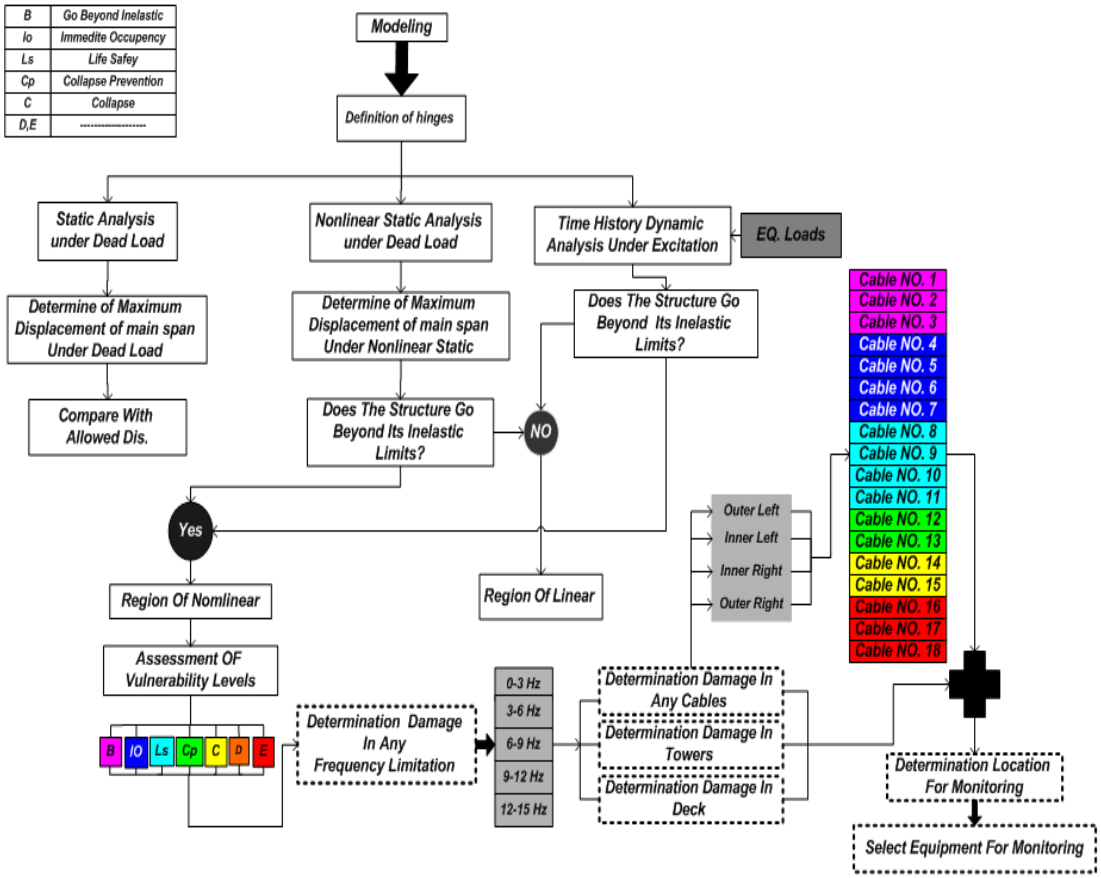

Fig. 3:The analysis steps for identifying the potential damages of cable-stayed bridge

III. THE MODEL PROPOSED FOR CABLE-STAYED BRIDGE

A. A.Cable model description

QINGZHOU Bridge which crosses Ming River (Fuzhou) has been selected for this research. The bridge span arrangements are 90+200+605+90+200 m. The elevation view of the bridge is shown in Fig.4.

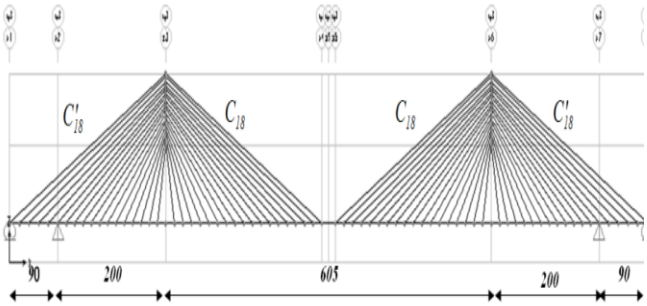

Fig. 4: Elevation view of QINGZHOU Bridge

The deck crosses aero dynamic section closely shaped with box steel girder of 25.1 m width and 2.8 m height with A=1.0175 m^2 and I=1.3232 m^4; where, A is Section Area and I is Moment Of Inertia. The bridge towers are A-shaped steel reinforced concrete towers with 175.5 m height, shown in Fig.5. The towers are connected to the deck by 18 cables in each side (inner cables and outer cables).The stayed cable is arranged as a two-vertical-plane system. The eight groups of cables are composed of 73–199 high-strength 7-mm wires.

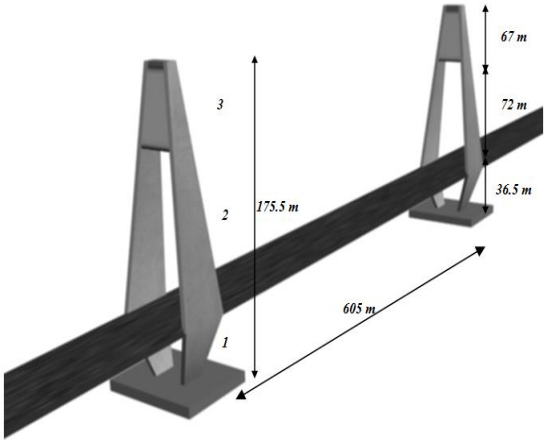

Fig. 5: 3D view of Bridge and A-Shape Tower

The specifications of different parts of towers and the material data of Sample Bridge have been extracted from reference [18] for modeling. One of the main objectives of this research is to determine the criteria for damage and nonlinear behavior of structure. Accordingly, the suggested model is sensitive to sag effect, interaction between axial load and bending moment in the main girders and towers, and large displacement effects. All these factors would result in nonlinear behavior of the structure.

B. MECHANICAL PROPERTIES AND INCLINATION OF CABLES

The cables are of main elements in all cable-stayed bridges. They are made up of steel with excellent mechanical properties such as a high tensile strength and a high elastic modulus. The cables are highly resistant against corrosion

having satisfactory fatigue strengths. While they are extremely strong, they are also very flexible making them appropriate for axial tension. However, they are weak against compression and bending forces. As a result, bridges with long span are vulnerable to the excitations such as strong winds and earthquakes, and therefore they need some special measures. Steel cables are very economical as they allow a slender and lighter structure which is still able to span long distances. Almost all steel wires are cylindrical shape with 3-7 mm diameter. The wires used in the cable-stayed bridges have the diameters up to 7 mm.

They carry the load of the main girder and transfer it to the towers. The cables in a cable-stayed bridge are all inclined, Figure 6. The actual stiffness of an inclined cable varies in accordance with the inclination angle (a), total cable weight (G) and cable tension force (T) [19]:

$$EA(eff) = EA/\{1+G^2EA\cos^2 a/(12T^3)\} \quad (1)$$

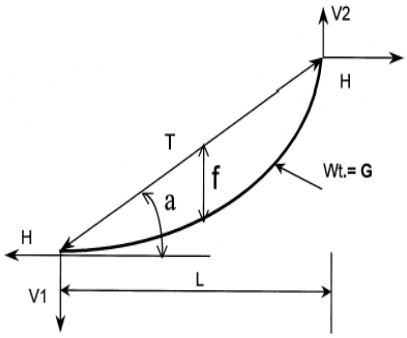

Fig. 6: An inclined cable

Where, E is Young's modulus and A is cross-sectional area of the cable. If the cable tension (T) changes from T1 to T2, the equivalent cable stiffness is defined as follows:

$$EA(eff) = EA/\{1+G^2EA\cos^2 a(T1+T2)/(24T1^2T2^2)\} \quad (2)$$

This equation is used in the present study to determine the cables sag effect.

C. Hinge definition

Concerning nonlinear analysis, the hinge should be defined according to the structural behavior of each element. In this research three types of hinge, cables, girders and towers, have been used for the elements. The hinge behavior is studied for the cables only under axial forces, the main girders connected to cables and the towers under the interaction of axial force and bending moment in two directions. These definitions have been considered as default status in nonlinear statistic procedure (NSP) and nonlinear dynamic procedure (NDP).The important point in nonlinear analysis is related to the force-deformation curve of members. In Fig.7 the Acceptance Criteria IO (Immediate Occupancy), LS (Life Safety) and CP (Collapse Prevention) values are deformations (displacements, strains, or rotations) that have been normalized by the same deformation scale factors used to specify the force-deformation curve, and are typically located between points, B and C, and, moreover, points B and C on the curve. The linear response beginning from A (unloaded component) to the yielding threshold B. Then, the linear response is observed at the reduced stiffness, from B to C, with sudden reduction in the lateral load resistance to D, response at reduced resistance to E, and final loss of resistance thereafter [20].

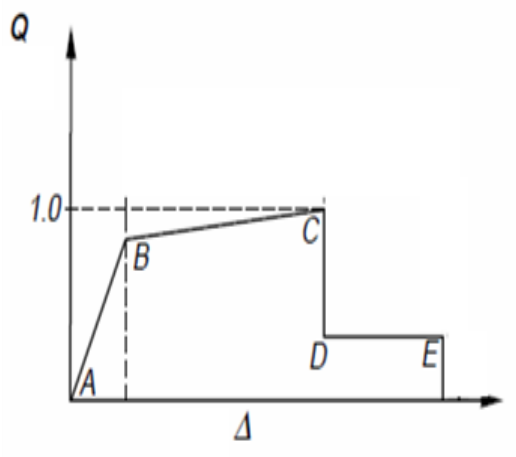

Fig. 7: Force – Displacement curve [20]

D. Selecting the earthquakes

In this research a procedure including normalizing, filtering and scaling is proposed in order to generalize dynamic time history analysis of cable-stayed bridges, Fig.2. In this way, in spite of applying various loads on the cable-stayed bridges and measuring different characteristics of strong ground motions, the damage patterns is recognized for each considered bridge. In this regard four earthquakes are chosen having the magnitudes of 6.4 ≤ Mw ≤ 7. The selected earthquakes are: **Kobe (STATION NO.2046, JAN 16, 1995), Big Bear (STATION NO.22561, JUNE 28,1992), El-Centro (IMPERIAL VALLEY, STATION NO.5054, OCT 15, 1979), Chi-Chi (SEP 20,99 , CHY028)**[21].

These records are selected out of a great of available records considering some major factors such as high magnitudes or epicenters intensities, near fault and far fault motions. In this way, the performance of bridge is controlled against weak to strong records to identify all possible damage/failure modes. Kobe earthquake is considered as the primary earthquake for analysis and the others as control samples for the proposed methodology. Accordingly, Kobe earthquake is firstly normalized to 1g. in longitudinal, transversal and vertical directions. Then, it is filtered in the frequency ranges of 0-15Hz. The frequency ranges are divided into the intervals of 0-3, 3-6, 6-9, 9-12, 12-15 to determine their relation with the dominant modes. These are used as input earthquakes of dynamic time- history analyses. The studied earthquakes are summarized in Table 1. Five frequency ranges have been assigned for the selected earthquakes. The damage is observed in the frequency range of 0-3 Hz. However, no damage is seen in other frequency ranges. Therefore, the input earthquake increases there. This increase has been 5 times the input earthquake in 3-6 Hz, 2 times in 6-9 Hz, 9 times in 9-12 Hz and 16 times in 12-15 Hz, Fig.1. This increase was about 2g which is an acceptable earthquake. In the next step, the frequency range of structural damage is determined. Fig. 8 shows the relation between frequency range and structural modes.

Table 1: The specifications of studied earthquakes

EQ.	Component X (g)	Component Y (g)	Component Up(g)	Duration (Sec)
Kobe 0-3 Hz.	0.90	0.95	0.72	26
Kobe 3-6 Hz.	0.34	0.36	0.70	26
Kobe 6-9 Hz	0.10	0.12	0.32	26
Kobe 9-12 Hz.	0.06	0.07	0.23	26
Kobe 12-15 Hz.	0.03	0.03	0.08	26
Big Bear	0.53	0.47	0.19	26
Chi Chi	0.82	0.65	0.34	25
El-Centro	0.60	0.77	0.42	25

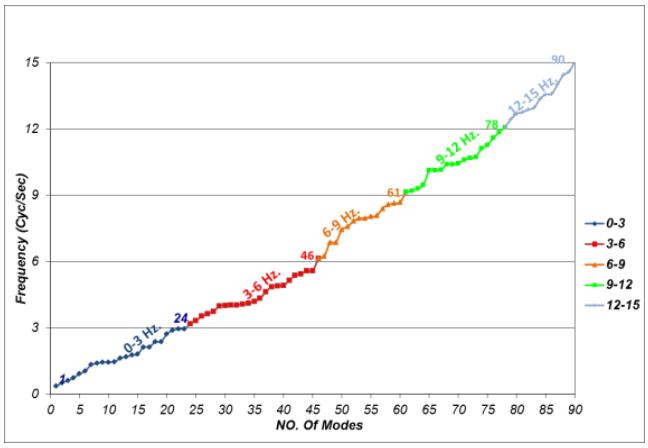

Fig. 8: The relation between the selected frequency range and involved modes

IV. Selecting the Proper Analysis Corresponding to Damage Diagnosis Feature

Here, linear statistic analysis, modal analysis, nonlinear statistic analysis and dynamic time history analysis have been conducted in order to evaluate the characteristics of different elements of bridge and their behaviors against external forces. These analyses are essential for determining the features sensitive to damage and their variation ranges. Therefore, the analyses are performed to evaluate the accurate condition of bridge and determine the points or features sensitive to damage.

The determined sensitive features are: 1) vertical displacement center of the main span; 2) root mean square of acceleration center of the main span; 3) lateral displacement of top of the towers; 4) vertical displacement of some points of the main girder of deck (area 3 located in region II and III, Fig. 20) near the towers; 5) cables strain. The details of all these features are defined in the following. By controlling the points accurately and determining the exact limitation for damage features it is possible to keep the structure in the linear and safe limitation throughout its life time and prevent the potential damages from occurring.

V. Damage Modes Assessment

The selected earthquakes are normalized and divided into different frequency ranges of 0-3, 3-6, 6-9, 9-12, 12-15 Hz. In this regard the behavior of the bridge is controlled under three directions in a small frequency range of about 24 modes. The potential excitation of special modes of the structure is identified causing minor damages to complete collapse.

At this stage, each filtered three directional records is applied on the structure as the input of nonlinear time history analysis to study the behavior of bridge. The analyses have been conducted after nonlinear static analyses of cable-stayed bridge under vertical dead loads.

If some parts of the bridge are not still in the elastic limitation, the applied record decreases by scaling; otherwise, it increases up to observing some damages in the bridge. The reasons of beginning the damage, its progress to the other sectors of the bridge and bridge collapse have been studied in each input frequency range by conducting more analyses. For this purpose, first, it is focused on the beginning stages of damage associated with different modes. Then, the propagation of damage in structural elements of the bridge, local failure and overall failure (collapse) would be identified. In the following the failure process is studied in different frequency ranges.

A. Damage in the Frequency Range of 0-3 Hz.

The structural damages are divided into 4 areas: left inner region (I), left outer region (II), right inner region (III), right outer region (IV) for better understanding the process.

Regarding the frequency range of 3.0 Hz, the structural damages are started with arriving some cables of regions (II) and (III) into inelastic limitation (B) (about 55% of cables in each region). As the analysis approaches, more cables of the four regions enter non-elastic limitation (B). After that, they do not exceed this limitation until the main span tower meets the boundary (B) as well. In this status, the damages are progressed in some cables of region III (50%B – 16% IO – 11% LS – 5 % C). This process is continued until the tower is out of elastic limitation; then, and the cables of region (III) experience damage expanding to the region (IV) and eventually (II). Meanwhile, both right and left towers also enter inelastic limitation and the damages are progressed up to their upper columns until stopping the analysis in Y direction due to the right tower failure because of excessive movement. Table 2 presents the damages occurred in the cables, towers and girders at the end of analysis. The overall damages of all members have been shown in Figure 9.

Table 2:The damage occurred in the cable- stayed bridge in the frequency range of 0-3 Hz.

Damage OF Cables					
Position	Time(Sec)	C-O-L	C-I-L	C-I-R	C-O-R
Front	11.12"	88% B	16% B - 77% IO	27% C - 72% E	100% E
Back	11.12"	88% B	16% B - 77% IO	5% B - 39% IO - 27% LS - 11% C - 16% E	88% B - 5.5% IO - 5.5 % LS

Damage OF Towers

Position	Tower	Time(Sec)	LEFT	RIGHT	Position	Tower	Time(Sec)	LEFT	RIGHT	Beam Under Deck (L)	Beam Under Deck (R)
FRONT	1	11.12"	–	–	BACK	1	11.12"	–	–	–	–
FRONT	2	11.12"	B	B	BACK	2	11.12"	–	B	B	B
FRONT	3	11.12"	–	B	BACK	3	11.12"	–	B	–	–

Damage OF Girders

Position	Time(Sec)	Span 1 (90m)L	Span 2(200m)L	Span 3(605/2m)L	Span 4(605/2m)R	Span 5(200m)R	Span 6 (90m)R
Front	11.12"	–	B	B	B	B	–
Back	11.12"	–	B	B	B	B	–

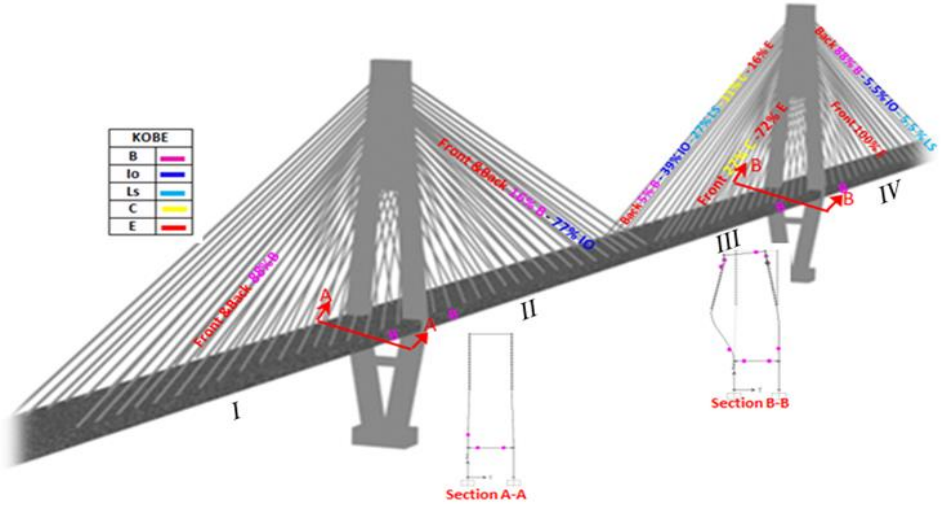

Fig9: Overall damages of all members

B. the Damage in the frequency range of 3-6 Hz.

The damages in the frequency range of 3-6 Hz. are started with entering some cables of regions II and III (about 61% of each of the regions II and III) the non-elastic limitation (B). As the analyses are continued, the damages are found in the regions I and IV as well. Therefore, the cables meet the border limitation (B). Continuing the analysis, no cable goes beyond the limitation until the girder of the main span is out of elastic limitation; then, the cables of the regions III and I are damaged. Eventually, the damage is occurred and progressed in the girders of region IV up to the stopping of analysis due to the mechanization of the girders of region I. No damage is happened in the towers in this frequency range.

Table 3 presents the damages of cables, columns and girders at the end of analysis. Overall damage of all members is shown in Fig. 10.

Table 3: The damage of cable- stayed bridge in the frequency range of 3-6 Hz.

Damage OF Cables

Position	Time(Sec)	C-O-L	C-I-L	C-I-R	C-O-R
Front	8.56"	94%B	94%B	50%B - 38%IO - 5% C	88%B
Back	8.56"	83%B - 5%IO - 5% C	94%B	38%B - 50%IO -5% LS	88%B

Damage OF Towers

Position	Tower	Time(Sec)	LEFT	RIGHT	Position	Tower	Time(Sec)	LEFT	RIGHT	Beam Under Deck (L)	Beam Under Deck (R)
FRONT	1	8.56"	–	–	BACK	1	8.56"	–	–	–	–
FRONT	2	8.56"	–	–	BACK	2	8.56"	–	–	–	–
FRONT	3	8.56"	–	–	BACK	3	8.56"	–	–	–	–

Damage OF Girders

Position	Time(Sec)	Span 1 (90m)L	Span 2(200m)L	Span 3(605/2m)L	Span 4(605/2m)R	Span 5(200m)R	Span 6 (90m)R
Front	8.56"	B/2(Collapse)	–	B	B	B/2	B/2
Back	8.56"	B/2(Collapse)	B/2	B	B	B/2	B/2

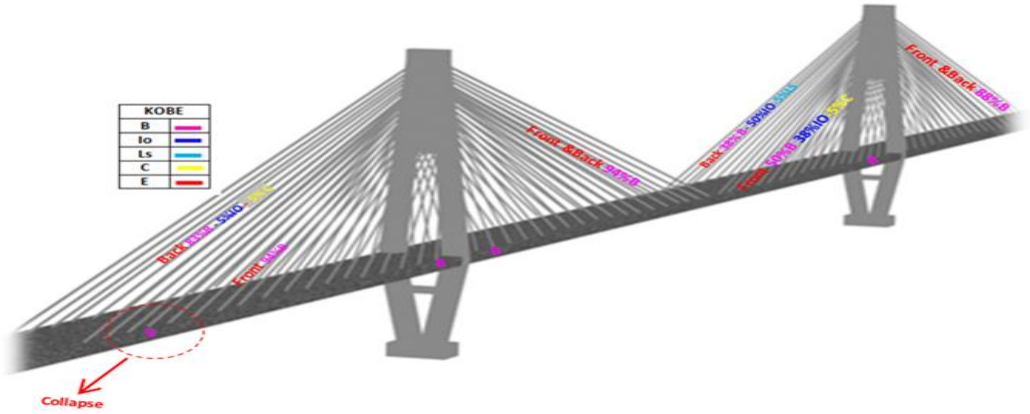

Fig. 10: Overall damages of all members

C. The damages in the frequency range of 6-9 Hz.

In this frequency range, the damages are started with entering some cables of the regions II and III (about 55% of cables of regions II and III) the limitation border (B). The analysis is continued and the damage of region III increases; and all cables and the girder of main span meet the border. In this condition the damage increases in region III. Eventually, some cables exceed the limitation C (27% B-22% IO -11% LS – 27% E) leading to the deck collapse. No damage is occurred in the towers in this frequency range. Table 4 presents the damages of cables, columns and girders at the end of analysis. The overall damage of all members is shown in Fig. 11.

Table 4: The damages of cable- stayed bridge in the frequency range of 6-9 Hz.

Damage OF Cables

Position	Time(Sec)	C-O-L	C-I-L	C-I-R	C-O-R
Front	26"	38%B	88%B	27%B - 22% IO - 16%LS - 22%E	44%B
Back	26"	38%B	88%B	27%B - 22% IO - 11%LS - 27%E	44%B

Damage OF Towers

Position	Tower	Time(Sec)	LEFT	RIGHT	Position	Tower	Time(Sec)	LEFT	RIGHT	Beam Under Deck (L)	Beam Under Deck (R)
FRONT	1	26"	-	-	BACK	1	26"	-	-	-	-
FRONT	2	26"	-	-	BACK	2	26"	-	-	-	-
FRONT	3	26"	-	-	BACK	3	26"	-	-	-	-

Damage OF Girders

Position	Time(Sec)	Span 1 (90m)L	Span 2 (200m)L	Span 3 (605/2m)L	Span 4 (605/2m)R	Span 5 (200m)R	Span 6 (90m)R
Front	26"	-	-	B	B	-	-
Back	26"	-	-	B	B	-	-

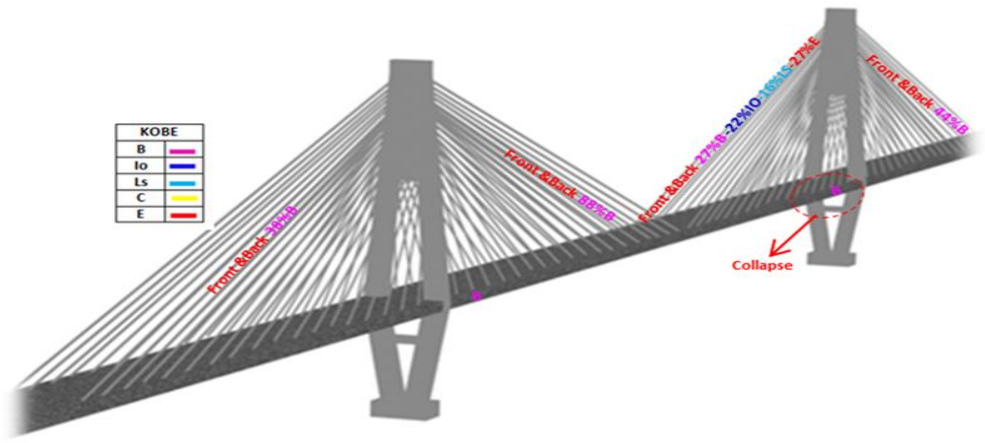

Fig. 11: Overall damage of all members

D. The damages in the frequency range of 9-12 Hz.

In this frequency range, the damages are started with meeting some cables (about 55%) of region II and III the border limitation (B). As the analysis is continued, the damages increase in these regions. Although all cables have not yet reached border limitation B, the girder of main span reaches this border. At this stage, the damage increases in the cables of region II (passing the border limitation C). The trend is progressed and the cables are damaged in region III exceeding the mentioned limitation border. Then damage is expanded into the region IV and some cables exceed the limitation C. In this stage the damages of girders meet region IV; the damages of right tower, under deck and top of the deck, meet the borders of B and IO limitations, respectively. Eventually, the analysis is stopped due to the deck collapse in region II.

Table 5 presents the damages of cables, columns and girders at the end of analysis. Overall damage of all members is shown in Fig. 12.

Table 5: The damages of cable- stayed bridge occurred in the frequency range of 9-12 Hz.

Damage OF Cables

Position	Time(Sec)	C-O-L	C-I-L	C-I-R	C-O-R
Front	26"	55%B - 11%IO	5%B - 83%E	100%E	11%B - 5%IO - 16% LS- 11%C - 55%E
Back	26"	55%B - 11%IO	5%B - 83%E	100%E	11%B - 5%IO - 16% LS- 11%C - 55%E

Damage OF Towers

Position	Tower	Time(Sec)	LEFT	RIGHT	Position	Tower	Time(Sec)	LEFT	RIGHT	Beam Under Deck (L)	Beam Under Deck (R)
FRONT	1	26"	–	IO/2	BACK	1	26"	–	IO/2	–	–
FRONT	2	26"	–	IO/2	BACK	2	26"	–	IO/2	–	–
FRONT	3	26"	–	–	BACK	3	26"	–	–	–	–

Damage OF Girders

Position	Time(Sec)	Span 1 $_{(90m)L}$	Span 2$_{(200m)L}$	Span 3$_{(605/2m)L}$	Span 4$_{(605/2m)R}$	Span 5$_{(200m)R}$	Span 6 $_{(90m)R}$
Front	26"	–	–	B	B	B	B/2
Back	26"	–	–	B	B	B	B/2

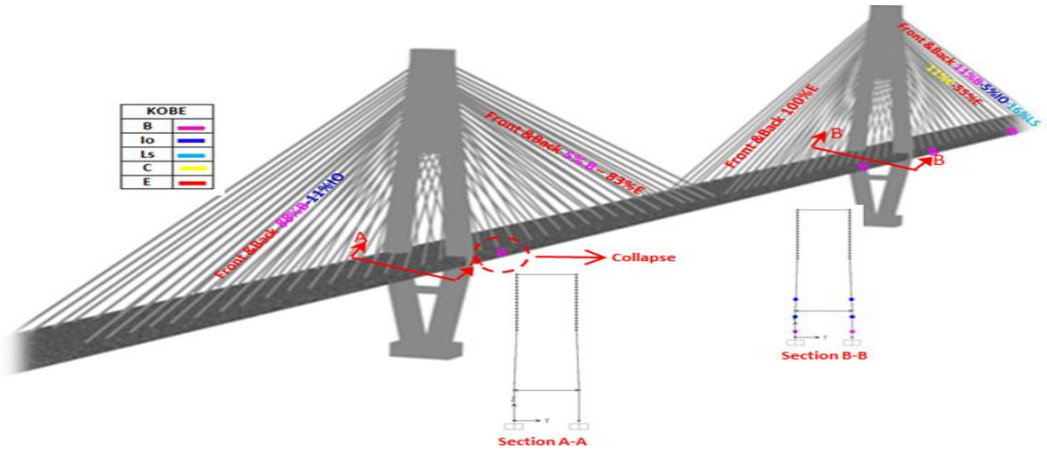

Fig. 12: Overall damage of all members

D. The damages occurred in the frequency range of 12-15 Hz.

The damage is started in the frequency range of 9-12 once some cables of region I and III (about 55%) reach the border of B limitation. Continuing the analysis, the damage increases in these regions. However, no cable exceeds B limitation until the girder of main span enters B limitation; the damage occurred in the cables of region III increases and exceeds C limitation. This condition continues and the damage is expanded into region II and passes C limitation. Then the damage is expanded to region I and some cables pass C limitation. In this stage the damages occurred in the girders of region I and the left towers, under and top of the deck, meet the border of B limitation. Eventually, the analysis is stopped due to deck collapse in the region III. Table 6 summarizes the damages of cables, columns and girders at the end of analysis. The overall damage of all members is shown in Fig. 13.

Table 6: The damage of cable- stayed bridge occurred in the frequency range of 9-12 Hz.

Damage OF Cables

Position	Time(Sec)	C-O-L	C-I-L	C-I-R	C-O-R
Front	15.62"	%B - 5%IO - 11%LS - 11%	5%LS - 5%C -89%E	83%E	39%B
Back	15.62"	3%B - 11%IO - 5%LS - 5%	5%IO - 11%C -83%E	83%E	45%B

Damage OF Towers

Position	Tower	Time(Sec)	LEFT	RIGHT	Position	Tower	Time(Sec)	LEFT	RIGHT	Beam Under Deck (L)	Beam Under Deck (R)
FRONT	1	15.62"	B/2	–	BACK	1	16"	B/2	–	–	–
FRONT	2	15.62"	B/2	–	BACK	2	16"	–	–	–	–
FRONT	3	15.62"	–	–	BACK	3	16"	–	–	–	–

Damage OF Girders

Position	Time(Sec)	Span 1 $_{(90m)L}$	Span 2$_{(200m)L}$	Span 3$_{(605/2m)L}$	Span 4$_{(605/2m)R}$	Span 5$_{(200m)R}$	Span 6 $_{(90m)R}$
Front	15.62"	–	B/2	B	B	–	–
Back	15.62"	–	B/2	B	B	–	–

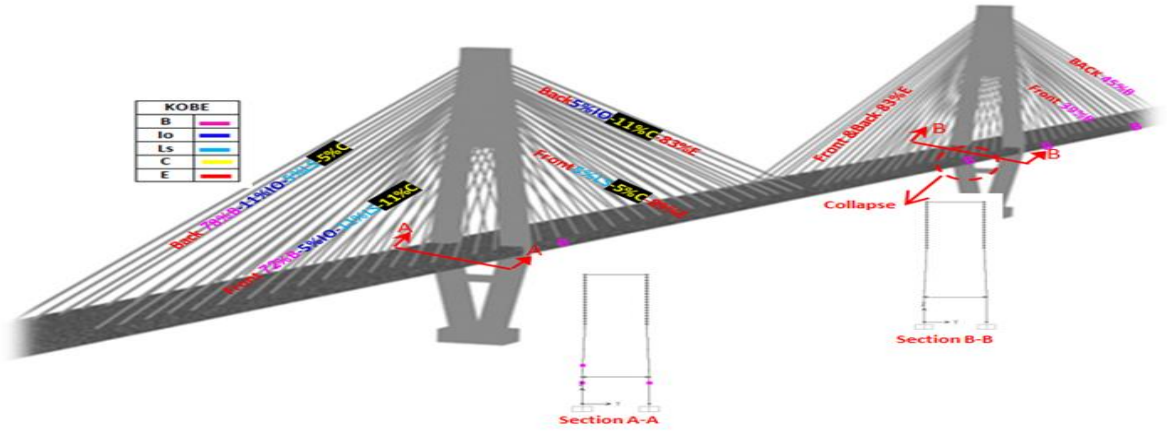

Fig. 13: Overall damage of all members

VI. THE FEATURES SENSITIVE TO DAMAGE

In this method, it is focused on studying the reasons of beginning the damage in different elements of the bridge, progressing of damage in other sectors of the bridge and occurring elements failure or bridge collapse in different frequency ranges in the regions I to IV. Then the features sensitive to damage and their displacements are determined in the given conditions.

The identified features are confined to certain frequency ranges. By the way, the cable stayed bridges health monitoring is possible in each performance level with evaluating the least bridge locations. Therefore, the detail damaging of the features sensitive to damage should be determined in different frequency ranges.

The features sensitive to damage are: displacement and root mean square of the center of main span acceleration, lateral displacement of the top of the towers, vertical displacement of some points of the main girder of the deck near the towers and cables strain.

The features sensitive to damage in the considered analysis and the progress of potential damages are studied in the following.

A. Controlling maximum displacement of the main span center

Vertical displacement of the main span center one of the most effective features in the trivial (small) damages to complete collapse of the cable stayed bridge. Its effect is widely observed in the cables of regions II and III. By continuing the analysis, the process approaches to other regions and elements and eventually leads to the overall collapse of the bridge. The damage progression and overall collapse are shown in Fig. 9-13 and tabulated in Tales 2-6. By conducting several analyses in the given frequency range, the boundary between safety and initial damage is well controlled based on the performance level. Since all The analyses are all dynamic time history and therefore the structural status can be controlled throughout the analysis. The displacement of the main span center exceeds the determined limitation (247cm, Fig. 14) in the frequency range of 0-3Hz. (Table 2). Therefore, one of the cables of region III meets failure boundary. As the analysis continues, the damage goes toward the cables of regions IV and II until stopping the analysis due to the large displacement in Y direction and eventually collapsing the right tower. Larger displacement of the main span center is needed for structural collapse in the frequency range of 3-6 Hz comparing to other ranges (Table 3). In this frequency range, as the displacement of the main span center exceeds the determined limitation (380cm, Fig. 14), one of the cables of region III reaches the failure boundary. Eventually, the damage progression toward region I lead to the failure of deck in this region. The displacement of the main span center exceeds the determined limitation (225cm, Fig. 14) in the frequency range of 6- 9 Hz (Table 4). Therefore, one of the cables of region III reaches failure boundary. By conducting the analysis, the damage progresses toward the cables of this region, 27% of which reaches the failure boundary eventually leading to the failure of deck (Fig. 16). If in this frequency range an earthquake causes the excitation modes of 46 – 61, the, damage is concentrated in the cables and deck. The displacement of the main span center exceeds the determined limitation (220cm, Fig. 14) in the frequency range of 9-12 Hz (Table 5). In this condition causes damage is occurred in the cables of region II and progressed in those of regions III and IV. Then the cables of region II

reach the failure boundary; eventually, the left tower is damaged leading to the deck collapse (Fig. 12).In the frequency range of 12-15 Hz (Table 6), the displacement of the main span center goes beyond the determined limitation (214cm, Fig. 14) and the cables of region III meet the failure boundary. By conducting the analysis the damage progresses towards the cables of regions II and III and exceed the failure boundary. This trend continues until the deck of the region III is collapsed due to the damage occurred in the columns of the right tower (Fig. 13). In the given bridge, this frequency range leads to the excitation modes of 78 to 90.

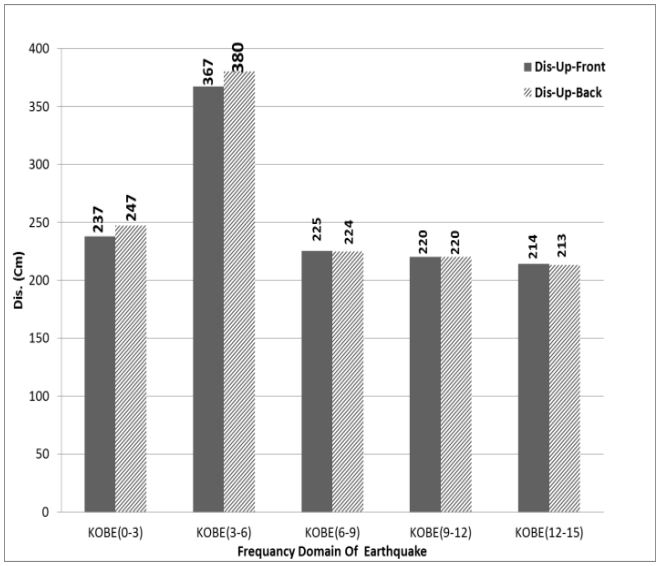

Fig. 14: Comparing the displacements of main span center in different frequency ranges

Fig. 14 shows the displacements of the main span center, regarding both front and back of the bridge, in all given frequency ranges. The cable stayed bridge is collapsed if the displacement of main span center goes beyond its minimum value (i.e. 213 cm in the frequency range of 12-15 Hz). Therefore, the excitation modes of 78 to 90 are dominant in this frequency range.

B. Controlling the acceleration root mean square of the main span center

The acceleration of main span center is another other feature sensitive to damage proposed for restricting the damage of cable stayed bridges. Therefore, the values of root mean square of main span center (front and back parts) are calculated and compared in different frequency ranges. Measuring the acceleration is more convenient (lower price) in comparison with that of displacement. Therefore, this feature is evaluated in different frequency ranges to determine the failure boundary of the bridge elements. Then damage to different frequency ranges and the safety boundary are examined precisely. According to Fig. 15, both acceleration components of the front and back of the deck are very close to each other. The root mean square values in the frequency range of 0-3 Hz are calculated for both front and back of the frames. As the root mean square value becomes higher than beyond 906 cm/s^2, the first cable of region III reaches the failure limitation. The trend goes toward region II, eventually leading to the left tower failure, Fig. 9. Finally, the bridge will collapse because of the failures occurred in the cables and towers.

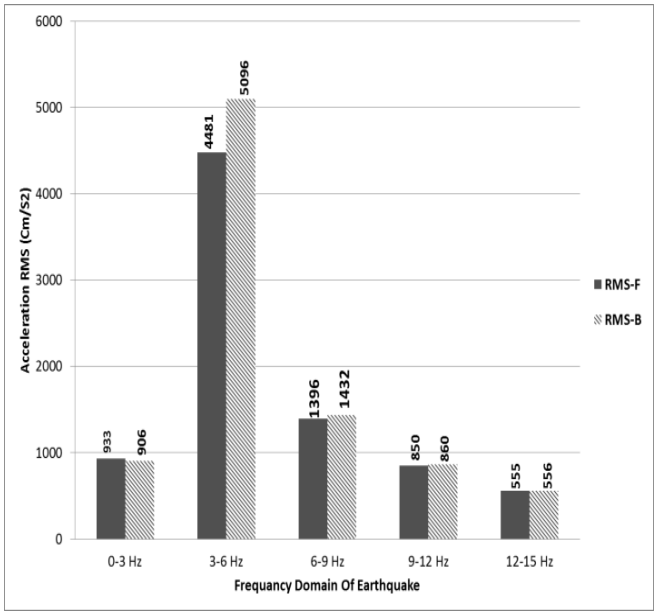

FIG15: The acceleration root mean square of the main span center for all given frequency ranges

In the frequency range of 3-6 Hz, as the root mean square value goes beyond 4481 cm/s^2 (Fig. 15), the cables of region III reach failure limitation and the trend progresses toward region I (Table 3).Meanwhile, the damage increases in the girders of region III. Eventually, the girders of region I are mechanized and the analysis is stopped. No damage occurs in the towers in the above mentioned frequency range; the bridge will collapse due to the collapse of cables and deck (Fig. 10). In this frequency range If an earthquake causes the excitation modes of 24-46, the condition will lead to the damage of cables and deck.

In the frequency range of 6-9 Hz (Table 4), as the root mean square value goes beyond 1394 cm/s2 (Fig. 15), the cables of region III reach failure limitation. By continuing the analysis, the damage progresses towards the cables; 27% of the cables go beyond the failure limitation and leading to the failure of deck (Fig. 11). The bridge will collapse because of the failure in the cables and deck. In this frequency range, if an earthquake causes the excitation modes of 46 – 61, the damage is concentrated in the cables and deck.

In the frequency range of 9-12 Hz (Table 5), as the root mean square value goes beyond 850 cm/s^2 (Fig. 15), the cables are stretched leading to damage of the cables of region II. This condition progresses toward regions III and IV. By continuing the analysis, the damage progresses toward the cables region II. Therefore, the cables go beyond the failure limitation, leading the trend to the failure of columns of the left tower. The process is continued up to the deck collapse in the region II (Fig. 12). The collapse of cables, towers and deck will lead to the bridge collapse. In this frequency range if an earthquake causes the excitation modes of 61-78, the damage is concentrated in the cables, towers and deck.

In the frequency range of 12-15 Hz (Table 6) the root mean square for both values are very close to each other in the front and back of the frames, about 556 cm/s^2- (Fig. 15). As the root mean square value goes beyond 556cm/s^2, the cables of region III reach failure limitation progressing toward the

cables of regions II and I. By continuing the analysis, the damage expands to the cables of regions II and III and goes beyond the failure limitation. However, the cables of region I reach the failure limitation without any changes in their conditions. Finally, this status damages the columns of right tower and the deck of region III will eventually collapse (Fig. 13).The failure of cables, towers and deck will lead to the bridge collapse. In this frequency range if an earthquake causes the excitation modes of 78-90, the damage is concentrated in the cables, towers and deck.

According to the results obtained in this research, the displacement of the main span center corresponds to its root mean square. Therefore, root mean square of the main span center can be used instead of its displacement in order to decrease the costs.

C. Controlling the lateral displacement of top of the towers

Based on the analyses conducted in the different frequency ranges, if the lateral displacement goes beyond the displacement of top of the towers in Y and X directions, severe damages are happened in different elements of the bridge. Therefore, besides identifying the damage limitation precisely, the displacement of top of the towers is controlled and determined to keep the performance level in the safe condition and prevent the damage from progressing.

Here, the damage is examined from two points of view: 1) when increasing in the lateral displacement of top of the towers leads to the deck failure; 2) lateral displacement of top of the towers leads to the damage to the cables, deck and deck columns.

The coincident lateral displacements of top of the right and left towers in X and Y directions are compared in all frequency ranges and presented separately in the Figs. 17- 18. According to Fig. 17, the lateral displacement of top of the right and left towers in direction X, causes the increase of cables strain in different regions of the bridge without any failure in the towers. This fact is discussed in the section concerned about the strain and its increase in the cables, Fig. 26.In the frequency range of 3-6 Hz, maximum lateral displacement of top of the towers in X direction is related to the right tower (i.e. about 84cm). As the lateral displacement of top of the towers in X direction goes beyond the maximum value (84cm), a cable of region III reaches the failure boundary and a cable of region I exceeds the failure boundary. Meanwhile, the damage occurred in the towers of region IV increases and eventually the analysis is stopped by mechanizing the girders of region I (Table 3). No damage is occurred in the towers in this frequency range. Therefore, the cables and deck are failed due to the large lateral displacement of top of the towers leading eventually to the bridge collapse. Therefore, the lateral displacement of top of the towers is restricted to prevent the potential damages and control the outer cables (regions I and IV) and deck. The frequency ranges of 6-9, 9-12 and 12-15 Hz have been studied in direction X for both right and left towers. According to the obtained results, if the lateral displacement of top of the towers goes beyond certain values (Fig. 16), only the cables, deck and tower's columns are damaged. However, no failure is occurred in the towers.

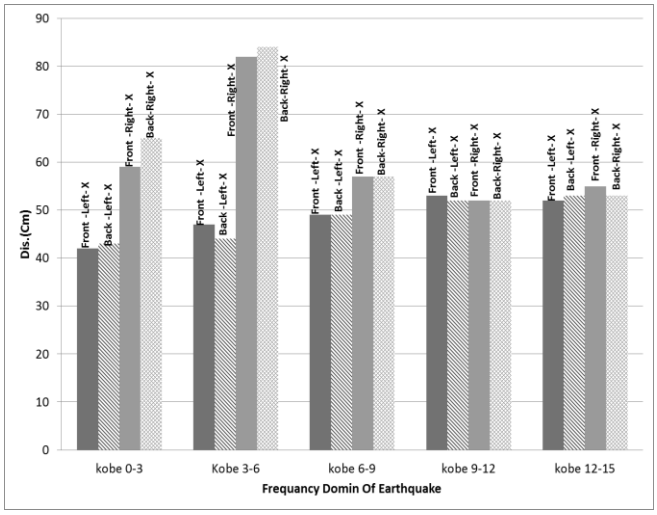

FIG16: Lateral displacements of top of the towers (X) for all given frequency ranges

The frequency ranges of 3-6, 6-9, 9-12 and 12-15 Hz in direction Y have been studied for both right and left towers (Fig. 17). Based on the obtained results, the lateral displacement of top of the towers is very small causing no damage to the bridge. However, in the frequency range of 0-3, the lateral displacement of top of the right tower is about 55cm. If the lateral displacement values of top of the towers in X and Y directions go beyond maximum (about 65cm), a cable of region III reaches the failure boundary.

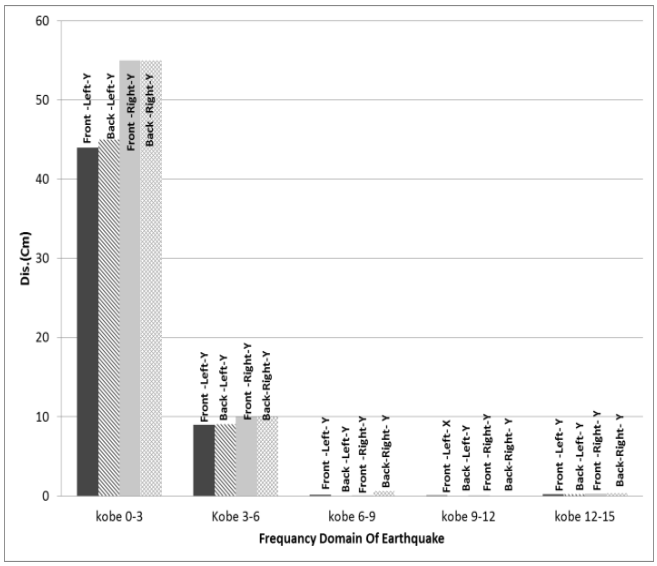

Fig. 17: Lateral displacements of top of the towers (Y) for all given frequency ranges

As the analysis continues, the damage progresses to the cables of regions IV and II. Dramatic increase in the lateral displacement of top of the towers in direction Y leads to the tower failure and eventually stopping the analysis. Therefore, in the frequency range of 0-3 Hz if an earthquake causes the excitation modes of 1-24, the lateral displacement of top of right tower in direction Y will increase. Eventually, the condition leads to tower failure. Fig. 18 shows the modes 16 and 19 along with the failure of right tower failure in direction Y.

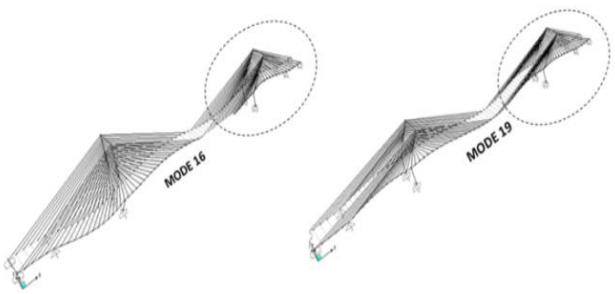

Fig. 18: The modes 16 and 19 in frequency range of 0-3 Hz.

Lateral displacement values of top of towers calculated in this research. By the way, the towers conditions are controlled; the damage is prevented from progressing to the other parts of the bridge; and the bridge is kept in the safe limitation.

Comparing the displacement of the main span center and lateral displacement of top of the towers, there will be three different scenarios for bridge damage:

1) Lateral displacement values of top of the towers in direction X exceed 85 cm and the displacement value of the main span center is over 3.5 m. The earthquake excitation will cause a great vertical displacement in the main girder. At the same time a great displacement is occurred in the towers in direction X. In this state the damages are mostly seen in the cables and deck of regions I and IV (Fig. 19-1) (Kobe earthquake in the frequency range of 3-6 Hz).

2) Lateral displacement of top of the towers is limited to 45 cm and the displacement of the main span center 2.20 m. Therefore, the earthquake excitation causes lower displacements of the main girder in the vertical direction and the towers in X direction, comparing to the first state. In this situation the damages are mostly seen in the cables and deck of regions II and III (Fig. 19-2) (Kobe earthquake in the frequency range of 0-3, 6-9, 9-12 and 12-15 Hz.).

3) Lateral displacement values of top of the towers are higher than 60cm and 55cm in X and Y directions, respectively. The earthquake excitation causes large displacements in the towers in X and Y directions. In this state the damage is ended to the towers failure (Fig. 19-3) (Kobe earthquake in the frequency range of 0-3 Hz.).

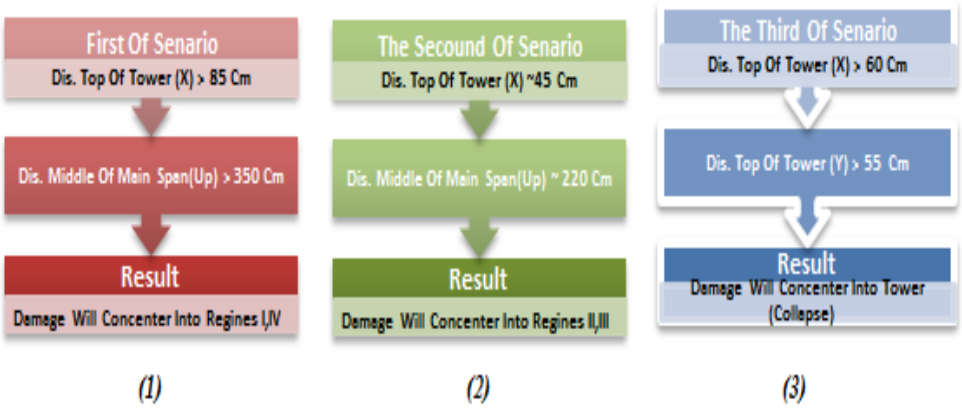

Fig. 19: Damage scenarios for different regions of bridge

D. Vertical displacement of some points of deck near the towers

The regions II and III are divided into three parts for better understanding of the collapse modes. These parts are: the cables near the tower; middle cables; and the cables near the main span center, Fig. 20. By conducting the analyses, deck collapse is seen in some of the frequency ranges. All collapses are observed in the region near the towers (region III). The exact safe limitation is determined by studying the vertical displacement of the failure points in the front and back frames. The safe limitation is shown in Figs. 21- 24.

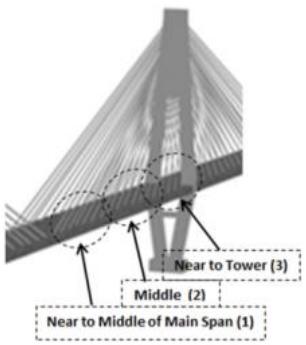

Fig. 20: Division the inner areas of cables

The vertical displacement of main span center as well as the failure points of area 3 (Fig. 20) should be considered in order to control the bridge condition more precisely. According to the damage progression shown in Figs. 14 -18, the damages and deck failure are mostly observed in area 3. These points are: point 228 in the left back frame in region II; point 726 in the left front frame in region II; point 573 in the right front frame in region III.

According to Fig. 21, the deck is failed in the frequency ranges of 9-12 and 12-15 Hz due to the vertical displacement of the back frame deck near the left tower (point 288), Figs. 12-13. However, by limiting the vertical displacement to 2m, all the cables will remain in the safe limitation.

The deck is failed in the frequency range of 6-9, 9-12 and 12-15 Hz (Figs. 11- 13) due to the vertical displacement of the back frame deck near the right tower (point 348, Fig. 22). Therefore, the boundary between safe limitation and damage initiation is about 2m for cables. If the boundary is higher than 2m, the cables will enter the failure limitation. Though in the frequency range of 0-3 Hz, exceeding this boundary value does not lead to the deck failure. The tower failure in Y direction leads to the deck failure in this frequency range, Fig. 9.

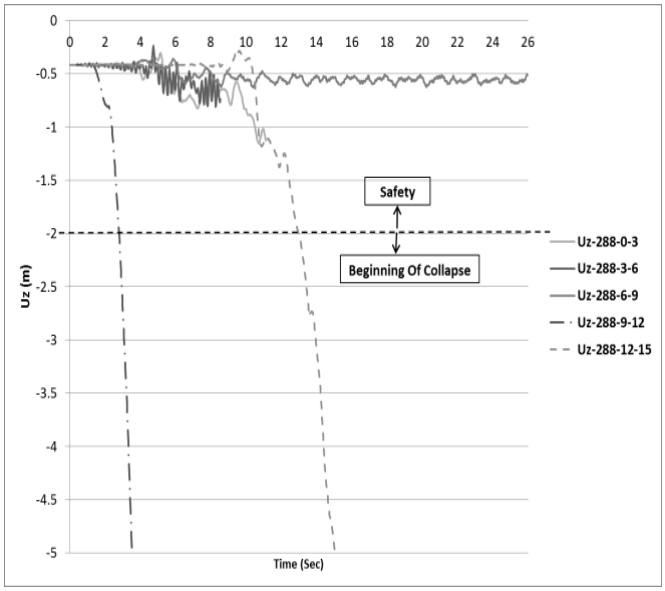

Fig. 21: Vertical displacement of point 288 near the towers

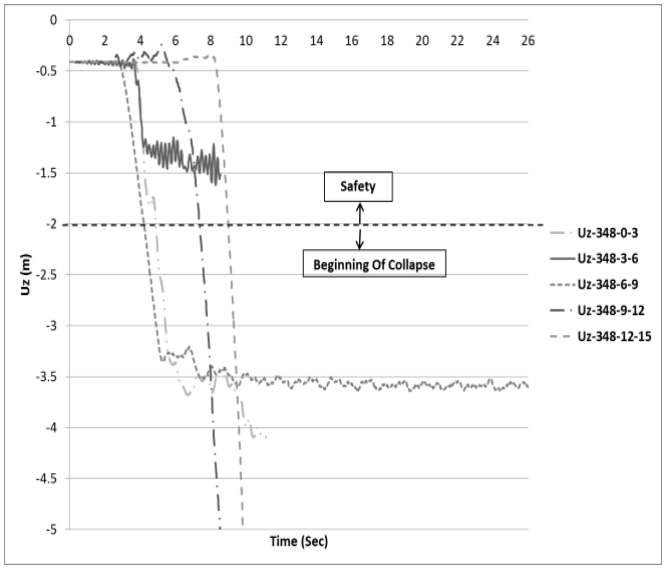

Fig. 22: Vertical displacement of point 384 near the towers
(Solid line = Safety; dotted line = Collapse initiation)
(Solid line = Safety & dotted line = Collapse initiation)

Regarding the back frame, the same study has been carried out on the front frame in the left and right sides of the bridge. According to the Figs. 23-24, a deck failure is occurred in the frequency ranges of 9-12 and 12-15 (Figs. 12- 13) at the point 726, in the front frame near the left tower. However, in the frequency range of 6-9, 9-12 and 12-15 Hz, a deck failure is observed in the front frame near the right tower, point 753, Figs. 11- 13. The events are shown in Figs. 23 and 24.
In the frequency range of 0-3 Hz, passing the boundary of 2m is not ended to the deck failure. However, the tower failure in Y direction leads to the deck failure, Fig. 9. According to Fig. 23, the allowable value of the back frame is lower than that of the right frame (Fig. 24). The points beyond the boundary of 2m are shown in dotted line in the above mentioned figures.

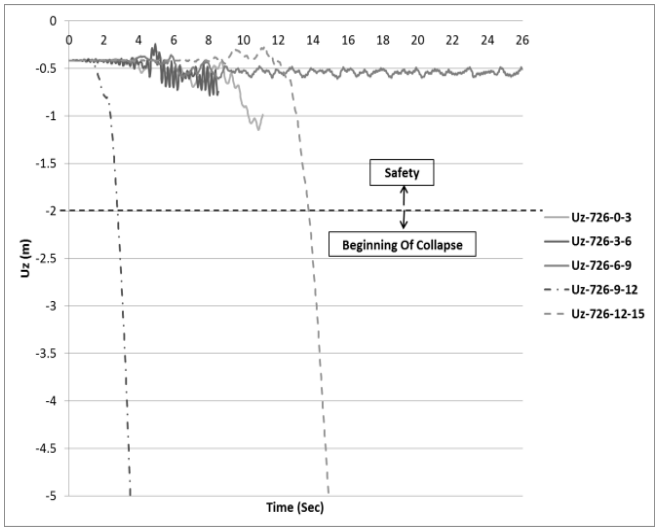

Fig. 23: Vertical displacement of point 726 near the towers

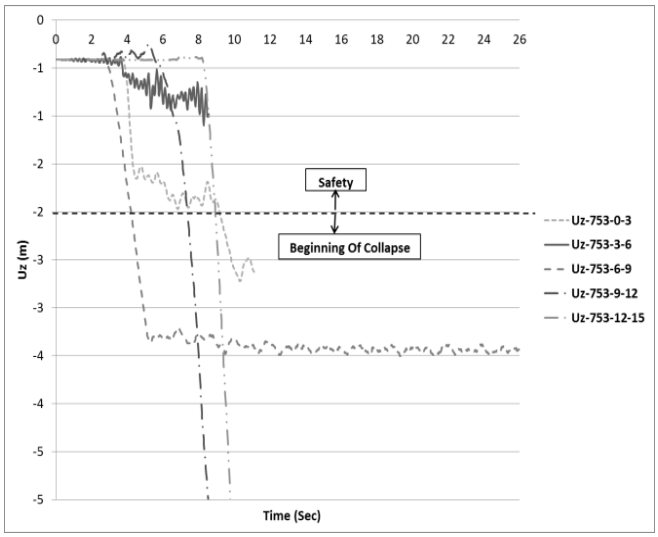

Fig. 24: Vertical displacement of point 753 near the towers
(Solid line = Safety; dotted line = Collapse initiation)
(Solid line = Safety & dotted line = Collapse initiation)

Lateral displacement of the main span center is determined in different frequency ranges, Fig. 14. The failure points of deck are detected in both right and left of the main span girder (area 3, Fig. 20). Therefore, the structure performance can be kept in the safe condition by simultaneous controlling of vertical displacement of the deck- located in area 3, near the tower- and the displacement of the main span center. In order to keep the vertical displacement in the safe condition, its value should be 2, lower than that of main span center.

E. Controlling the cables strain

Sag effect is one of the factors that causes inelastic condition in the cable stayed bridges. The strain is controlled in each cable to determine its exact limitation. In this phase the damage can be prevented progressing and the cables are kept in the safe condition. The equivalent analytical equation has been used to obtain the real values of strain, registered by strain gage in the earthquakes. Accordingly, the sag effects of the cables are calculated using elasticity module using Equation 1. Then, the strain values are calculated in each cable with respecting to the sag effect. Sag effect has been calculated according to equation (3) by using equivalent elasticity module. Then the strain of each cable is obtained considering sag effect and inclines [11].

$$E_{eq} = \frac{E}{1 + \frac{(L_0\gamma)^2(\sigma_1 + \sigma_2)}{24\sigma_1^2\sigma_2^2} E} \quad (3)$$

Where, E is the elasticity module of cable; L0 is horizontal projected length of the cable; γ is specific gravity of the cable; σ_1 is primary tension stress; and σ_2 is the tension stress of cable. The damage limitation, damage process and performance level of cables are determined using tension stress equation. The performance level is achieved according to the values of strain and damage of the longest cable located in region III (cable 61) in all frequency ranges, Fig. 25.

Fig. 25 shows the changes of strain-stress for the cable number 61 in the frequency ranges of 0-3 Hz and 12-15 Hz. The cable is studied precisely in different performance levels in order to obtain their exact corresponded values of strain.

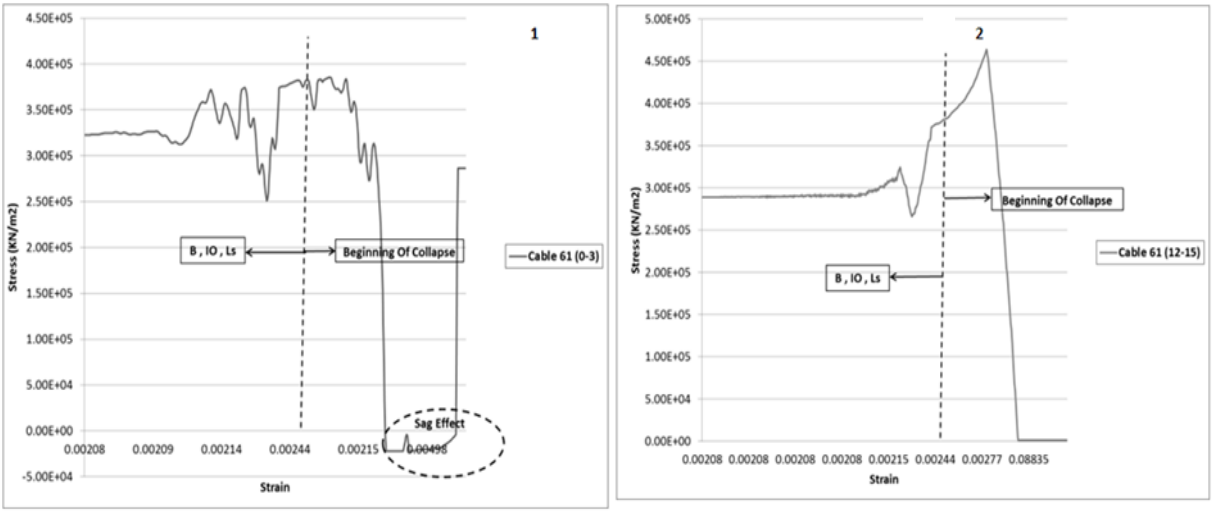

(1) (2)

Fig. 25: The performance levels of cable 61 in the frequency ranges of 0-3, 12-15 Hz.

In the frequency range of 0-3 Hz. (Fig. 25-1) the stress and consequently bearing capacity of cable decrease as the strain increases (over 0.0024); it goes beyond the limitation C. According to the figure, if the cables incline (at the end of analysis) the stress increases again perhaps due to the residual strain. When two ends of the cable move towards each other and causes the inclination of cable, the stress becomes zero. However, the length of cable increases, some parts of which is elastic and some inelastic. This condition is clearly seen in the frequency range of 12-15Hz. After passing the failure boundary, with the increase of strain the bearing capacity decreases until the stress reaches zero (Fig. 25-1).The performance levels are all calculated easily and accurately as the conducted analyses have been dynamic time history. The strain values, obtained from analyses, are 0.0020, 0.0022 and 0.0024 for limitations B, IO and LS, respectively. The performance levels are presented as C and E points in Fig. 7 for the strain values greater than 0.0024.The limitations corresponding to different strain values have been determined. The strain values have been calculated for different regions and shown in Fig. 26. According to this figure, in the frequency range of 0-3Hz, the cables of region III reach the limitations C and E exceeding the strain of 0.0024 (9- 11.12 sec.) and stopping the analysis at 11.12 sec. Fig. 9 shows the damage values of the cables of front frame in region III as 27% C and 72% E. Fig. 26-1 shows the cables 56 to 61, exactly corresponded to Fig. 9.

The cables of front frame in region III have been studied in the frequency range of 3-6 Hz. In this condition only one cable goes beyond the failure boundary. The damage values of cables are 5% C, 38% IO, 50% B, shown Fig. 10. These values confirm the results obtained in this research. All cables are at the maximum strain of 0,002, excluding the cable number 30 which is higher than that, Fig. 26-2. In the frequency range of 6-9Hz, the cables number 30, 33, 35 and

39 of the front frame in region III reach failure limitation and their strain values exceed 0.0024, Fig. 26-3. Their damage values 16% LS, 22% IO, 27% B and 27% E, respectively, Fig. 11. These values well confirm the illustration of Fig. 33. In the frequency range of 9-12Hz, all cables of front frame in region III reach failure limitation with the strain values over 0.0024. The condition for cable number 22 is shown in Fig. 26-4. According to Fig. 12, the damage value of cables is 100% E that confirms the results illustrated in the figure. In the frequency range of 12-15Hz, all cables of front frame in region III reach the collapse limitation (with the strain values over 0.0024) except the cables 30, 33 and 35 that remain in the elastic limitation, Fig. 26-5. The illustration of this figure is confirmed by the obtained damage value of cables (83% E), shown in Fig. 13.

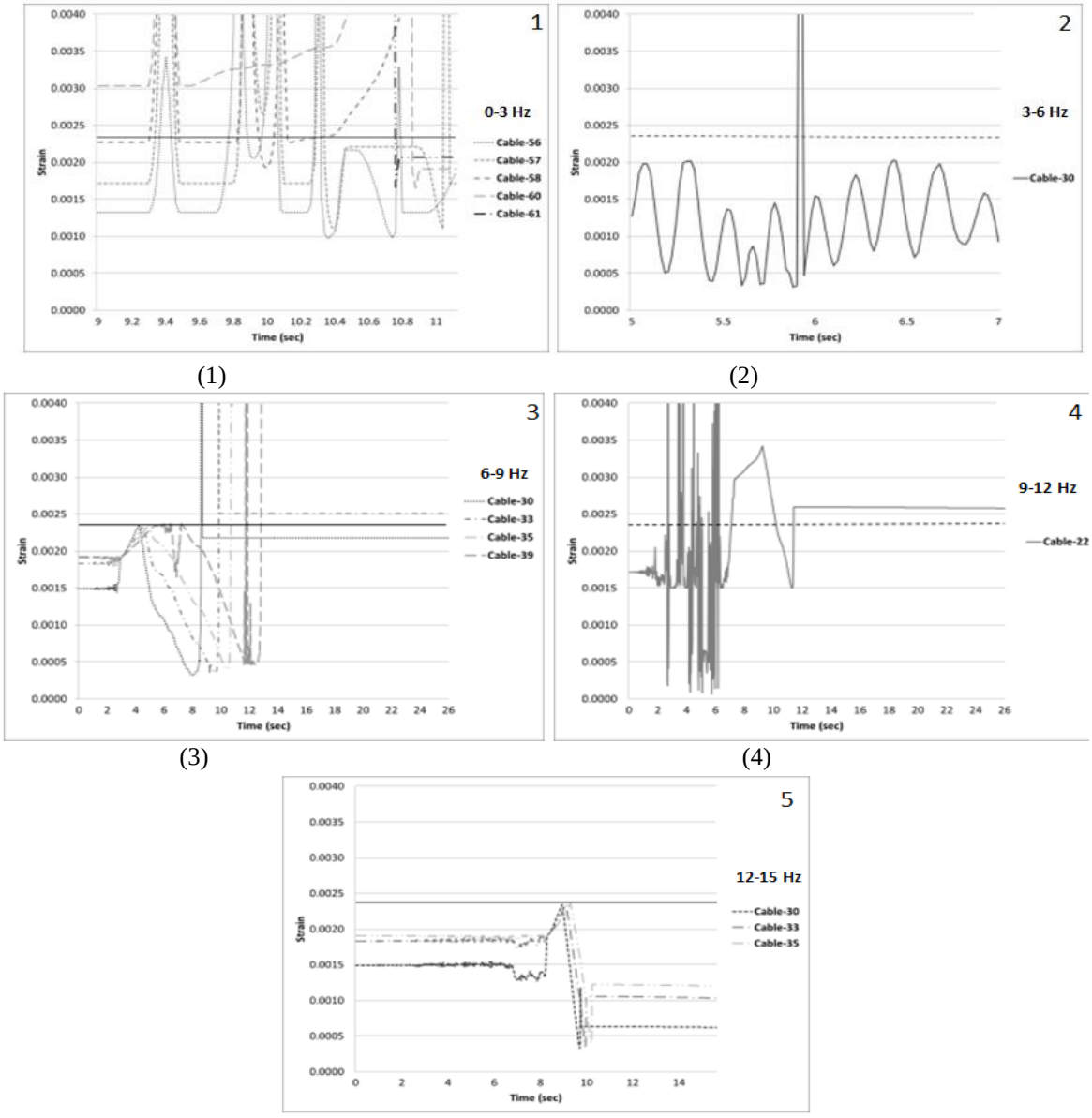

Fig. 26: Comparing the Strains of Right Inner Cables in Different Frequency Ranges

The amount of damage occurred in each cable can be determined by controlling the strains. If cable strain exceeds the identified value (0.0024), the inelastic limitation can be determined according to the defined performance level. Therefore, the structure is kept in the safe limitation and the damage extension is prevented by controlling the inelastic limitation precisely.

VII. Determining and Controlling the Features Sensitive to Damage

The analyses have been conducted using Kobe earthquake in the frequency ranges of 0-3, 3-6, 6-9, 9-12 and 12-15Hz. The features sensitive to damage have been determined. These features are: lateral displacement of top of the towers, vertical displacement of some points of main girder of deck near the towers and cables strain. The suggested methodology should be controlled by some other control sample earthquakes as well. For this purpose, Big Bear, Chi-Chi and El-Centro earthquakes are selected having the acceleration spectrums different from that of Kobe earthquakes.. Their acceleration spectrums for X directions are illustrated in Fig. 27.

If the results obtained from these earthquakes are corresponded to that of Kobe earthquake, it is inferred that the proposed methodology is acceptable. Accordingly, the structure can be kept in the safe limitation. Moreover, the damage extension is prevented by controlling the features sensitive to damage.

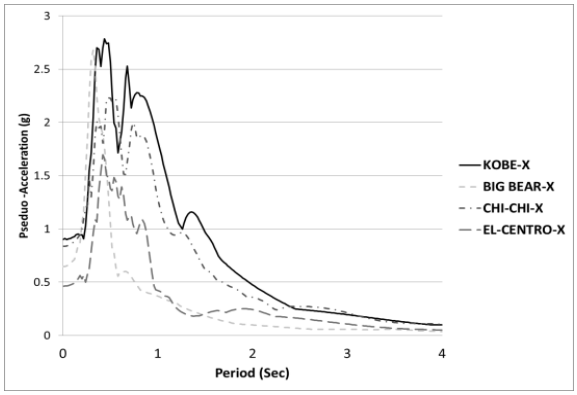

Fig. 27: Acceleration spectrum X

Table 7 presents the results of analyses conducted on the control sample earthquakes as well as the features sensitive to damage. According to the results obtained for Big Bear earthquake, the displacement of main span center, lateral displacement of top of the tower and root mean square of acceleration are similar to that of Kobe earthquake in the frequency range of 3-6Hz (Figs. 14-17).

Table 7: The analysis results of control sample earthquakes

EQ.	Dis. Middel Span (m)	Dis. Left Tower Top (Cm)	Dis. Right Tower Top (Cm)	RMS - X (Cm/S^2)	RMS - Y (Cm/S^2)	RMS - Up (Cm/S^2)	RMS (Cm/S^2)	Dominant frequency (Hz.)
BIG BEAR /Front	3.13	72(x)-2.5(y)	54(x)-0.18(y)	2792	1345	851	3214	(3-6)
BIG BEAR/Back	3.13	57(x)-2.5(y)	54(x)-0.18(y)	3649	1345	824	3975	(3-6)
CHI CHI/Front	2.49	45x)-68(y)	43(x)-71(y)	4296	1262	1137	4620	(0-3)
CHI CHI/Back	2.5	46(x)-68(y)	45(x)-71(y)	2008	1263	1132	2628	(0-3)
EL-CENTRO/Front	2.6	57(x)-76(y)	56(x)-77(y)	1403	1170	1006	2086	(0-3)
EL-CENTRO/Back	2.64	56(x)-76(y)	57(x)-77(y)	2856	1171	1058	3263	(0-3)

According to the obtained results, the damage caused by Big Bear earthquake is exactly the same as that of Kobe event in the frequency range of 3-6 (Fig. 10). In this frequency range the damage progresses to the cables of region I causing the failure of deck.

Concerning the Fourier domain of Big Bear earthquake, the maximum domain is in the frequency range of 3-6 Hz, Fig. 28.

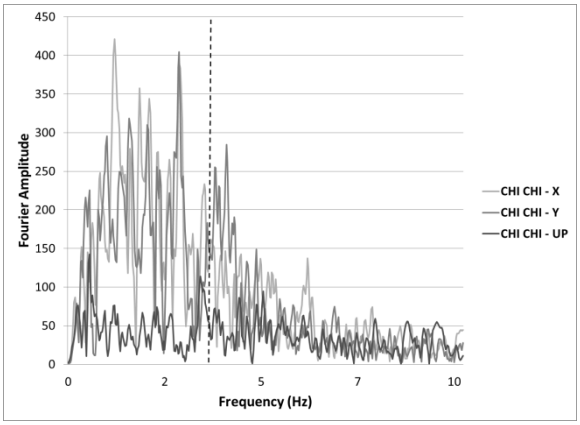

Fig. 28: Fourier Domain of Big Bear Earthquake

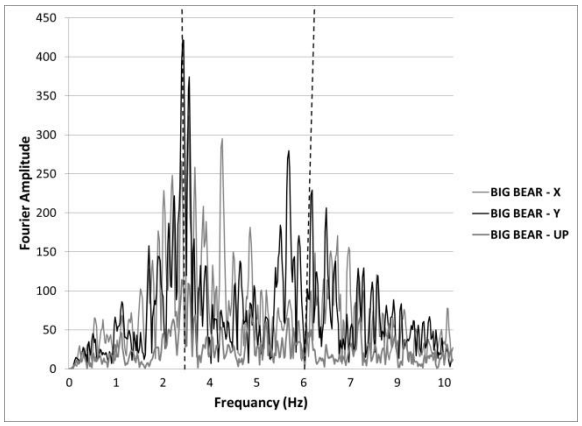

Fig. 29: Fourier Domain of Chi-Chi Earthquake

Based on the results obtained for Chi-Chi and El-Centro earthquakes (Table 7), lateral displacement of top of the towers in Y direction is similar to that of Kobe earthquake in the frequency range of 0-3 Hz (Figs. 16- 17). The displacement of the main span center is exactly the same as that of Kobe earthquake in the frequency range of 0-3Hz. (Fig. 14) in which the damage eventually progresses to the deck, girders under deck and towers` columns.

Regarding the Fourier domains of Chi-Chi and El-Centro earthquakes, maximum domain is in the frequency range of 0-3Hz, The fact has been presented in Fig. 29 for Chi-Chi earthquake. Therefore, if an earthquake is in a frequency range of Kobe earthquake, the expected damages are exactly the same as that of Kobe.

VIII. Conclusion

In this paper a new methodology is proposed to identify the features sensitive to damage based on different frequency ranges of input earthquakes. In the suggested method, it is likely to and examines the beginning phase, progression and extension of damage can be identified and controlled. Therefore, the cable stayed bridges can be practically kept safe by restricting the potential damages. By applying this methodology along with complementary control systems, the potential damages can be prevented from occurring in the cable stayed bridges.

In this methodology, first, the earthquake is normalized to 1g in the vertical, transversal and longitudinal directions and used as the input for nonlinear dynamic time history analyses. Then, each 3-component record is divided into frequency ranges of 0-3, 3-6, 6-9, 9-12 and 12-15. Each frequency range covers 10 to 25 frequency modes of the bridge. The acceleration increased in the given frequency range up to damage occurred in the bridge. At this stage, by identifying the failure modes, all damage stages are controlled, from damage initiation to the bridge collapse, in each frequency ranges. Finally, the excitation mode which causes different potential damages to the bridge is found. Then, the features sensitive to damage and their changes are determined by examining the failure modes of the bridge. The features, considered in this study are: 1) vertical displacement of main span center; 2) root mean square of the acceleration of main span center; 3) lateral displacement of top of the towers; 4) vertical displacement of some points of the main girder of the deck (area 3 located in regions II and III) near the towers; 5) strain of cables. In the proposed methodology, the exact boundaries of the recognized features for damage initiation, extension of damages, and finally collapse conditions of the bridge are quantifiable.

In order to verify the proposed methodology, other earthquake records such as the Big Bear, the Chi-Chi, and the El Centro earthquake records are examined and their results are compared with those concern to the Kobe earthquake, extensive analyses show that the proposed methodology is robust and very strong to recognize a few specific features of a cable-stayed bridge in order to determine the bridge vulnerability and its controlling to prevent damages in different parts of cable stayed bridges due to various sources of excitations.

REFERENCES

[1] *Brownjohn J. M. W., Bocciolone M, Curami A, Falco M, Zasso A, Humber Bridge full-scale measurement campaigns 1990-1991. JWEIA 52 185-218, 1994.*

[2] *Barr I. G., Waldron P., Evans H. R., Instrumentation of glued segmental box girder bridges. Monitoring of Large Structures and Assessment of their Safety.IABSEColloquium Bergamo, 1987.*

[3] *Lau CK, Wong KY, Design, construction and monitoring of three key cable-supported bridges in Hong Kong. Proc 4th International Kerensky Conference on Structures in the new millennium, Hong Kong, 105-115, 1997.*

[4] *Leitch J, Long A E, Thompson A, Sloan T D, Monitoring the behavior of a major box-girder bridge. Structural Assessment Based on Full and Large-Scale Testing, BRE Garston 212-219, Butterworth, 1987.*

[5] *Chang, K. C., Mo, Y. L., Chen, C. C., Lai, L. C. and Chou, C. C. 2004. Lessons Learned from the Damaged Chi-Lu Cable-Stayed Bridge. Journal of Bridge Engineering, ASCE, Vol. 9, No. 4,343-352.*

[6] *Farrar, C.R., and James, G. H. Ⅲ, 1997, System Identification from Ambient Vibration Measurements on a Bridge, Journal of Sound and Vibration, Vol. 205(1), pp. 1-18.*

[7] *Huang, C.C., and Loh C.H., 2001, Nonlinear Identification of Dynamic System Using Neural Networks, Journal of Computer-Aided Civil Infrastructure Engineering, Vol.16, pp. 28–4.1*

[8] *Nazmy A.S., Abdel-Ghaffar A.M., 'Three-Dimensional Nonlinear Static Analysis of Cable-Stayed Bridges', Computers and Structures, 34, pp. 257-271, 1990.*

[9] *Nazmy, A. S., and Abdel-Ghaffar, A. M. (1990a). Non-linear earthquake-response analysis of long-span cable-stayed bridges: Theory. EarthquakeEngrg.andStruct. Dyn., 19, 45–62.*

[10] *Abdel-Ghaffar, A. M., and Nazmy, A. S. (1991). 3-D nonlinear seismic behavior of cable-stayed bridges. J. Struct. Engrg, ASCE, 117(11), 3456–3476.*

[11] *Nazmy A.S., Abdel-Ghaffar A.M., 'Three-Dimensional Nonlinear Static Analysis of Cable-Stayed Bridges', Computers and Structures, 34, pp. 257-271, 1990.*

[12] *Fleming, J. F., and Egeseli, E. A. (1980). Dynamic behavior of a cable stayed bridge. Earthquake Engrg.andStruct. Dyn. 8, 1–16.*

[13] *Nazmy, A. S., and Abdel-Ghaffar, A. M. (1990a). Non-linear earthquake- response analysis of long-span cable-stayed bridges: Theory. EarthquakeEngrg.andStruct. Dyn., 19, 45–62.*

[14] *Lee, Z. K., Chen C. C., Chou, C. C. and Chang, K. C. 2006. Finite Element Analysis of Ambient Vibration Signal of Stay Cables. Journal of Chinese Institute of Civil and Hydraulic Engineering, Vol. 18, No. 2, 279 - 288.*

[15] *Loh, C. H., and Ho, R. C. (1990). Seismic damage assessment based on different hysteretic rulers. Earthquake Engrg.andStruct. Dyn. 19, 753–771.*

[16] *Betti, R., Abdel-Ghaffar, A. M., and Nazmy, A. S. (1993). Kinematic soil-structural interaction for long-span cable-supported bridges. Earthquake Engrg.andStruct. Dyn., 22(5), 415–430.*

[17] *Mohammad Hashemi Yekani. Monitoring systems optimization and provide application of software for bridges and tall structures. PH.D. Thesis, Department of Civil Engineering, Research and Science Branch Islamic AzadUniversity,Tehran,Iran;2017.*

[18] *Wei-Xin Ren1 and Makoto Obata2. ELASTIC-PLASTIC SEISMIC BEHAVIOR OF LONG SPAN CABLE-STAYED BRIDGES'JOURNAL OF BRIDGE ENGINEERING / AUGUST 1999.*

[19] Tang, M. Cable-Stayed Bridges. *Bridge Engineering Handbook.*Ed.Wai-Fah Chen and LianDuan CRC Press, 2000.

[20] *Federal Emergency Management Agency, FEMA-356.Prestandard and commentary for seismic rehabilitation of buildings. Washington (DC);2000.*

[21] *Peer Strong Motion Database Record. Processing By Pacific Engineering*